PRODUCTION OF CHARM AT HERA

C.D. HILTON

Department of Physics and Astronomy, The University of Manchester, Manchester M13 9PL, UK

Results from the study of the production of charm quarks in positron-proton collisions at HERA are reviewed. Charm is identified in the H1 and ZEUS detectors in the form of D^*, J/ψ or $\psi(2S)$ mesons. Inelastic and elastic production mechanisms are studied.

1 Introduction

Charm is produced in positron-proton collisions at HERA predominantly as a $c\bar{c}$ pair in the current system. Production can occur in inelastic collisions, in which colour is transferred from the proton so that the proton breaks up, or in the case of J/ψ and $\psi(2S)$ vector mesons also in diffractive interactions, in which no colour is transferred and the proton can remain intact (elastic interaction) or dissociate.

Models for the direct inelastic production of charm are based on the photon-gluon fusion mechanism, where the positron radiates a photon which participates in the hard interaction with a gluon from the proton to form a $c\bar{c}$ pair. The hard interaction is calculable in perturbative QCD, and the production is clearly sensitive to the gluon content of the proton. To achieve a colourless J/ψ state at least one further gluon must be involved in the interaction. In the colour-singlet model [1,2] the radiation of a gluon from a $c(\bar{c})$ line to form a colourless $c\bar{c}$ state is part of the hard interaction, whilst in the colour-octet model [3] the transition from the coloured $c\bar{c}$ state produced in the hard sub-process proceeds non-perturbatively.

Charm is also produced in collisions in which the photon does not participate directly in the hard sub-process, but is 'resolved', that is, a parton from the photon is involved leaving a spectator photon-remnant. The resolved photon contribution is significant in photo-production, that is where the exchanged photon has a negative mass-squared, Q^2, less than about 1 GeV^2, but not in Deep Inelastic Scattering (DIS) at higher Q^2.

In the model of diffractive production of J/ψ and $\psi(2S)$ mesons in which the interaction is mediated by a 'soft pomeron' [4], a cross-section proportional to $W_{\gamma p}^{\delta}$, with $\delta = 0.32$, is predicted, where $W_{\gamma p}$ is the centre-of-mass energy in the γp collision. Ryskin et al have developed a model in which the pomeron is replaced by gluon ladders which can be calculated in perturbative QCD by assuming that the charm quark mass offers a hard scale [5]. In this case the cross-section is proportional to the square of the gluon density of the proton at Bjorken $x \approx m_{J/\psi}^2/W_{\gamma p}^2$, and a much steeper rise with $W_{\gamma p}$ than in the soft pomeron case is predicted for current parametrizations.

The results presented are based upon data recorded by the H1 [6] and ZEUS [7] detectors during 1994 and 1995, when positrons with energy 27.5 GeV and protons of energy 820 GeV were collided head-on in HERA.

2 Inelastic Production of Charm

2.1 D^* Photo-production [8,9]

D^* mesons are identified in the H1 and ZEUS detectors by the decay $D^{*+} \rightarrow D^0\pi^+$, in the kinematic region where the transverse momentum of the D^* meson is greater than 2.5 GeV (3.0 GeV in the ZEUS analysis) and the laboratory rapidity between -1.5 and 1.0. Events with $Q^2 > 4$ GeV^2 are rejected by insisting that the scattered electron is not found in the main part of the detector.

In the visible kinematic region described above, the cross-section measurements are found to be insensitive to the choice of parton density parametrizations. The photo-production cross-section $\sigma(\gamma p \rightarrow c\bar{c}X)$ is inferred by extrapolating from the restricted kinematic range to the total ep cross-section for D^* production, using the fragmentation fraction $B_{c\rightarrow D^*} = 0.260$ [10] and assuming a photon flux as given by the Weizsäcker-Williams Approximation [11]. The result is shown in figure 1 where the inner error bars represent the combined statistical and systematic errors, and the outer error bars include the large uncertainty

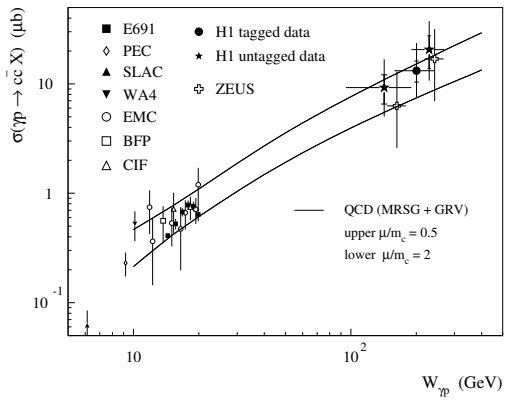

Figure 1: Total charm photo-production cross-section as a function of $W_{\gamma p}$, including results from fixed-target experiments[12], and predictions of NLO QCD calculations[13] with MRSG [14] and GRV-G HO [15] parton density parametrizations. H1 'tagged' events refer to those where the scattered e^+ was detected in the low angle electron tagger.

in the extrapolation which arises due to the possible choices of parton density parametrizations. The prediction of a NLO QCD calculation [13] is shown for two extreme values of the renormalization scale as indicated.

A strong rise of the photo-production cross-section of charm with $W_{\gamma p}$, with respect to earlier results from lower energy collisions, is observed.

2.2 D^* and D^0 Production in DIS[16,17]

The production of D^* and D^0 in events in which the scattered electron has been identified, where $10 < Q^2 < 100$ GeV^2, has been studied with the H1 detector. In addition to the D^* decay channel above, D^0 are sought directly via their decays to $K^-\pi^+$. Extrapolating from the visible D cross-sections to the full $c\bar{c}$ cross-sections introduces less uncertainty than in the photo-production case. The cross-sections are shown in figure 2 in the form of $F_2^{c\bar{c}}$, the charm contribution to the proton structure function, where

$$\frac{d^2\sigma^{c\bar{c}}}{dxdQ^2} = \frac{2\pi\alpha^2}{Q^4 x}\left[1+(1-y)^2\right] F_2^{c\bar{c}}\left(x,Q^2\right). \quad (1)$$

A large increase in $F_2^{c\bar{c}}$, with respect to lower energy data at higher Bjorken x, is observed.

NLO QCD predictions based on various parametrizations of the proton structure are below the measured values, with a calculation based on a fit to the H1 F_2 measurements providing the closest estimate. The measured ratio $F_2^{c\bar{c}}/F_2$ is found to be compatible with being constant over the visible kinematic range, with an average value of $0.237 \pm 0.021 \pm^{0.043}_{0.039}$.

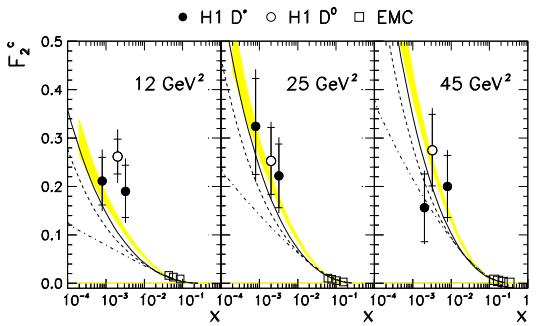

Figure 2: $F_2^{c\bar{c}}$ measurements from H1 D^0 (full circles), H1 D^* (open circles) and EMC (squares) analyses. Inner error bars are statistical, outer total. Compared to NLO calculations[18] based on GRV-HO [19] (full line), MRSH [20] (dashed line), MRSD0' [21] (dash-dotted line), H1 F_2 measurements[22] (shaded stripe).

2.3 J/ψ Photo-production[23,24]

J/ψ mesons are identified by their decays to lepton pairs. The cross-section measurements are restricted to the range in z ($\equiv E_{J/\psi}/E_\gamma$ in the proton rest frame) between 0.3 and 0.9 where the contributions from diffractive production and resolved photon events are small. For comparison with NLO QCD calculations in the colour-singlet model, cross-section determinations are restricted to the kinematic region $p_t(J/\psi) > 1$ GeV.

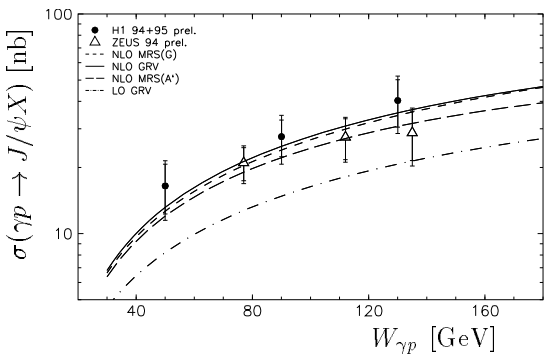

Figure 3: Direct photo-production cross-sections for J/ψ, compared to NLO and LO QCD calculations in the colour-singlet model[2] based on the parton density parametrizations MRSG [14], GRV-LO [25], MRSA' [26]. Inner error bars statistical, outer total.

Figure 3 shows the direct inelastic photo-

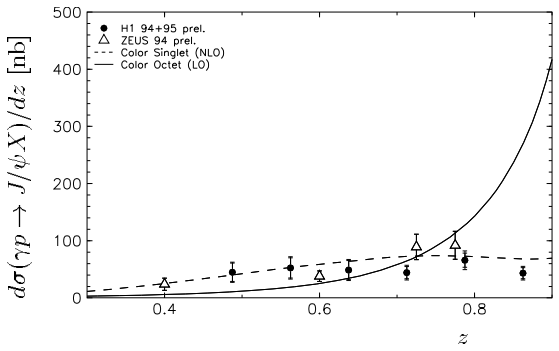

Figure 4: Differential photo-production cross-section for J/ψ in the variable z, compared to predictions of the colour-singlet and colour-octet models[3].

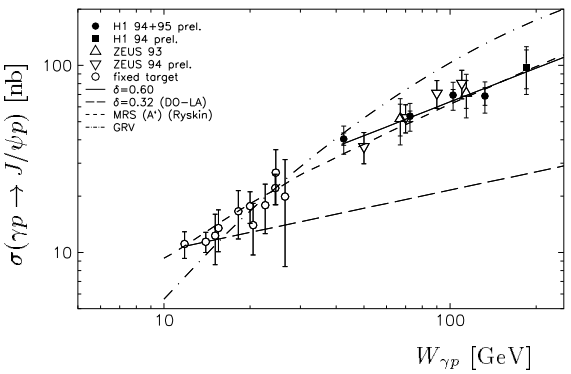

Figure 5: Elastic photo-production cross-section for J/ψ vs $W_{\gamma p}$. Inner error bars statistical, outer total. Parametrizations of the $W_{\gamma p}$ dependence as $W_{\gamma p}^{0.6}$ and $W_{\gamma p}^{0.32}$, and calculations in according to the Ryskin model for gluon density functions as shown. Included are results from fixed target experiments[29]

production cross-section of J/ψ as a function of $W_{\gamma p}$ for $z < 0.8$, with predictions from NLO QCD calculations based on various proton structure parametrizations and with a LO QCD calculation. A strong rise in the cross-section with $W_{\gamma p}$ is observed which, in the model used, reflects the rising gluon content of the proton towards low x. The results are not sensitive enough to distinguish between different parametrizations of the gluon content of the proton.

As can be seen in figure 4, the differential cross-section in z is also well reproduced by the calculation based on the colour-singlet model, but contains no indication of the sharp rise towards high z which is predicted in the colour-octet model if the normalization is chosen to fit the CDF data[27].

3 Diffractive Production of Charm

3.1 J/ψ Photo-production[23,24]

Cross-sections for the elastic interaction $\gamma p \to J/\psi p$ are measured by isolating a sample of events where no energy deposit is found in the detector other than that associated with the decay products of the J/ψ meson, and estimating the remaining inelastic contamination. A strong rise of the cross-section with increasing $W_{\gamma p}$ is observed (figure 5), which is significantly beyond that expected for interactions mediated by a soft pomeron ($\delta = 0.32$). Rather, a value $\delta = 0.60$ provides a better fit to the H1 and ZEUS measurements.

A good description of the rise in the cross-section is given by calculations in the Ryskin model[28]. In figure 5, curves are shown for two parametrizations of the gluon density. The absolute normalization of the calculations is not reliable, so that only the shapes should be used to distinguish between different parametrizations.

The b slope for the elastic interaction $ep \to J/\psi p$ is measured using a fit of the form $d\sigma/dp_t^2 \propto e^{-bp_t^2}$ to the data with $p_t^2 < 1$ GeV^2. Values $b = 3.7 \pm 0.2 \pm 0.2$ GeV^{-2} for $30 < W_{\gamma p} < 90$ GeV and $b = 4.6 \pm 0.3 \pm 0.3$ GeV^{-2} for $90 < W_{\gamma p} < 150$ GeV are obtained (H1 preliminary).

3.2 J/ψ Production in DIS[30,31]

By seeking events where, in addition to the decay products of the J/ψ, a scattered positron is found, the elastic interaction $\gamma^* p \to J/\psi p$ has been studied at an average Q^2 of about 16 GeV^2. Comparing the cross-sections as measured by the H1 and ZEUS experiments with those from fixed target experiments, a rise with $W_{\gamma p}$ similar to that seen in photo-production events is observed. The measurements with the H1 detector show a Q^2 evolution of the cross-section compatible with $1/(Q^2 + m_{J/\psi}^2)^n$ with $n = 1.9 \pm 0.3$ (stat.).

3.3 $\psi(2S)$ Photo-production[32]

Clear signals for $\psi(2S)$ are seen by searching for the decay to $J/\psi\pi^+\pi^-$ in the H1 detector where the J/ψ subsequently decays to a lepton pair, and insisting that no further charged particles are identified (figure 6). The acceptance is limited to the kinematic region $z > 0.95$, where a ratio for the

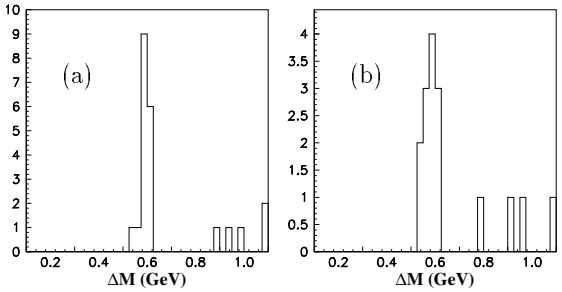

Figure 6: (a) Distribution of $\Delta M \equiv M_{\mu^+\mu^-\pi^+\pi^-} - M_{\mu^+\mu^-}$ for four-prong events where a muon pair is found satisfying $2.8 < M_{\mu^+\mu^-} < 3.4$ GeV. Unshaded region: all combinations found, shaded region: events used for cross-section calculation. (b) Same for decay $J/\psi \to e^+e^-$.

photo-production cross-sections, $\sigma(\psi')/\sigma(J/\psi) = 0.16 \pm 0.06$ at $W_{\gamma p} = 80$ GeV is measured. This ratio appears energy independent when comparing to measurements from other experiments[33] at $W_{\gamma p} < 20$ GeV.

4 Conclusions

The production of charm quarks in e^+p-collisions at HERA has been studied by identifying charm in the form of D, J/ψ and $\psi(2S)$ mesons. All photo-production cross-sections are found to rise steeply with increasing $W_{\gamma p}$. This characteristic is well described by models based on perturbative QCD in which the rise reflects the increase in the gluon content of the proton towards low x.

Acknowledgments

I acknowledge the members of the H1 and ZEUS collaborations, whose work has contributed to the attaining of the results presented here. Also the organizers of the 28th ICHEP.

References

1. M.Krämer et al.,*Phys.Lett.*B348, 657 (1995)
2. M.Krämer,*Nucl.Phys.*B459, 3 (1996)
3. M.Cacciari,M.Krämer,DESY 96-005 (1995)
4. A.Donnachie,P.V.Landshoff,*Phys.Lett.* B348, 213 (1995); ibid.B296, 227 (1992)
5. M.G.Ryskin,*Z.Phys.*C57, 89 (1993)
6. H1 Collab.,DESY 96-001 (1996)
7. ZEUS Collab.,DESY 95-193 (1995)
8. H1 Collab., contribution pa02-088 ICHEP, Warsaw, 1996
9. ZEUS Collab., contribution pa02-051 ICHEP, Warsaw, 1996
10. OPAL Collab.,CERN-PPE-94/217 (1994) LEP Collab.,CERN-PPE-96/017 (1996)
11. C.F.Weizsäcker,*Z.Phys.*88, 612 (1934) E.J.Williams,*Phys.Rev.*45, 729 (1934)
12. CIF Collab.,*Phys.Rev.Lett.*43, 414 (1979); BFP Collab.,*Phys.Rev.Lett.*45, 682 (1980); SLAC HFP Collab.,*Phys.Rev.*D30, 1 (1984); EMC Collab.,*Z.Phys.*C35, 1 (1987); *Nucl.Phys.* B213, 31 (1983); *Phys.Lett.*B167, 127 (1986); PEC Collab.,*Phys.Lett.*B187, 437 (1987); E691 Collab.,*Phys.Rev.Lett.*65, 2503 (1990); WA4 Collab.,*Phys.Lett.*B94, 113 (1980)
13. S.Frixione et al.,*Phys.Lett.*B348, 633 (1995); *Nucl.Phys.*B454, 3 (1995)
14. A.D.Martin et al.,RAL-94-055 (1994)
15. M.Glück et al.,*Phys.Rev.*D45, 3986 (1992)
16. H1 Collab., contribution pa02-089 ICHEP, Warsaw, 1996
17. ZEUS Collab., contribution pa02-031 ICHEP, Warsaw, 1996
18. S.Riemersma et al,*Phys.Lett.*B347, 143(1995)
19. M.Glück et al.,*Z.Phys.*C53, 127 (1992)
20. A.D.Martin et al.,*Phys.Rev.*D50,6743 (1994)
21. A.D.Martin et al.,*Phys.Lett.*B306,145 (1993)
22. H1 Collab.,*Nucl.Phys.*B470, 3 (1996)
23. ZEUS Collab., contribution pa02-085 ICHEP, Warsaw,1996
24. H1 Collab., contribution pa02-047 ICHEP, Warsaw,1996
25. M.Glück et al.,*Phys.Rev.*D46, 1973 (1992)
26. A.D.Martin et al.,*Phys.Lett.*B354,155 (1995)
27. CDF Collab.,*Phys.Rev.Lett*69, 3704 (1992)
28. M.G.Ryskin et al.,DTP-95-96 (1995),revised Feb 1996
29. E687 Collab.,*Phys.Lett.*B316, 197 (1993); E401 Collab.,*Phys.Rev.Lett.*48, 73 (1982); FTPS Collab.,*Phys.Rev.Lett.*52, 795 (1984)
30. H1 Collab.,*Nucl.Phys.*B468, 3 (1996)
31. ZEUS Collab., contribution pa02-028 ICHEP, Warsaw, 1996
32. H1 Collab., contribution pa02-086 ICHEP, Warsaw, 1996
33. EMC Collab.,*Nucl.Phys.*B213, 1 (1983); NA-14 Collab.,*Z.Phys.*C33, 505 (1987); E401 Collab.,*Phys.Rev.Lett.*50, 302 (1983)